Acta Geodyn. Geomater., Vol. 22, No. 4 (220), 501–511, 2025
DOI: 10.13168/AGG.2025.0036
journal homepage: https://www.irsm.cas.cz/acta

ORIGINAL PAPER

CO-SEISMIC DEFORMATION OF THE 6 FEB 2023 TURKEY EARTHQUAKES AND THEIR IMPACT ON NORTHERN EGYPT: A GNSS AND SENTINEL-1 InSAR-BASED STUDY

Rehab TAHA [1)] *, Magda H. FARHAN [1)], Ali M. BASHA [1)], Mahmoud GOMAA [2)] and Mohamed SALEH [2)]

[1)] *Civil Engineering Department, Faculty of Engineering, Kafrelsheikh University, Kafrelsheikh, 33511, Egypt*
[2)] *Geodynamics Department, National Research Institute of Astronomy and Geophysics (NRIAG), Helwan, Cairo, Egypt.*

**Corresponding author's e-mail:* rehab.taha1998@gmail.com

ARTICLE INFO

Article history:
Received 8 July 2025
Accepted 6 November 2025
Available online 13 November 2025

Keywords:
InSAR
Earthquake activities
Time Series
Turkey Earthquakes

ABSTRACT

Earthquakes in the Mediterranean region can cause significant damage in northern Egypt, making it essential to study these events and assess their potential impacts. This work investigates crustal deformation associated with one of the largest earthquakes of the last century—the 6 February 2023 Turkey doublet. Such earthquakes can affect areas hundreds of kilometers and potentially influence Egypt, particularly in the northeastern Mediterranean region. To evaluate the impact of the 6 February earthquakes, GNSS observations and Interferometric Synthetic Aperture Radar (InSAR) data were utilized. GNSS observations along northern Egypt were analyzed, including time series before, during, and after the earthquakes. The results show that in Turkey, the earthquake's effects are evident at the MERS station, which is the closest to the epicenter, while other stations exhibit little or no influence. In Egypt, the observed displacements during the earthquake appear to be related to local movements rather than to the Turkish events. Furthermore, no aftershocks associated with the 6 February earthquakes were detected in Egypt. Overall, the findings indicate that the 6 February 2023 earthquakes did not produce significant crustal deformation in northern Egypt. Instead, the primary hazard to Egypt may be related to potential tsunami waves generated by such earthquakes rather than ground displacements.

INTRODUCTION

Currently, understanding crustal deformation along active faults is crucial for conserving resources and lives. One of the major natural disasters, earthquakes, has been studied for over 200 years, yet our understanding of them remains limited. The time and location of the impending earthquake's triggering are yet unknown (Liu et al., 2024). Due to the sudden release of massive earthquake energy, people have no possibility of being protected from the risk. In the last decade, only a few devastating earthquakes have caused trillions of dollars in damage, hundreds of fatalities, and thousands of injuries (Li et al., 2023; Sandwell et al., 2011). Turkey experienced a devastating event in 2023 when two large earthquakes struck the country. The devastation caused by these earthquakes was extensive. The earthquakes in Turkey may have an impact on Egypt's northern coastline. Therefore, it is necessary to assess the impact of the large earthquakes that struck the northern region of Egypt along the eastern Mediterranean Sea (Potin et al., 2016).

The 2023 Turkey earthquake sequence occurred in the Gaziantep region of southern Turkey. On 6 February 2023, at 01:17 UTC, a powerful earthquake with a moment magnitude of Mw 7.8 struck the area. According to the United States Geological Survey, the epicenter was located at 37.174°N, 37.032°E, with a hypocentral depth of 17.9 km (Zahradník et al., 2023). Approximately nine hours later, a Mw 7.5 earthquake struck near Kahramanmaraş, about 95 km north of the Mw 7.8 epicenter (37.203°E, 38.024°N, depth 10.0 km) (Chen et al., 2022). It is extremely rare for two large earthquakes (Mw > 7.5) to occur on adjacent faults within just a few hours apart (Wang et al., 2023). The Mw 7.8 event was the most destructive earthquake in Turkey since the 1939 Erzincan earthquake (Mw 7.9) (Delouis et al., 2023). As illustrated in Figures 1 and 2, the North Anatolian Fault Zone (NAFZ) represents the most active structural feature in Turkey and is one of the most seismically significant strike-slip faults in the world (Gunaydin et al., 2023). The unprecedented sequence of earthquakes caused direct infrastructure losses exceeding $34 billion, severely damaging residential buildings, industrial facilities, bridges, transportation networks, harbors, earth structures, and lifelines in densely populated regions (Özkan et al., 2023). The Mw 7.8 earthquake initiated along the North Anatolian Fault (NAF) and ruptured bilaterally along the East Anatolian Fault Zone (EAFZ). The Mw 7.6 earthquake occurred along the Çardak Fault (CF), propagating in an east–west direction (Farr et al., 2007; Melgar et al., 2023).

Cite this article as: Taha R, Farhan MH, Basha AM, Gomaa M, Saleh M: Co-seismic deformation of the 6 Feb Turkey earthquakes and their impact on northern Egypt: A GNSS and Sentinel-1 InSAR based study. Acta Geodyn. Geomater., 22, No. 4 (220), 501–511, 2025. DOI: 10.13168/AGG.2025.0036

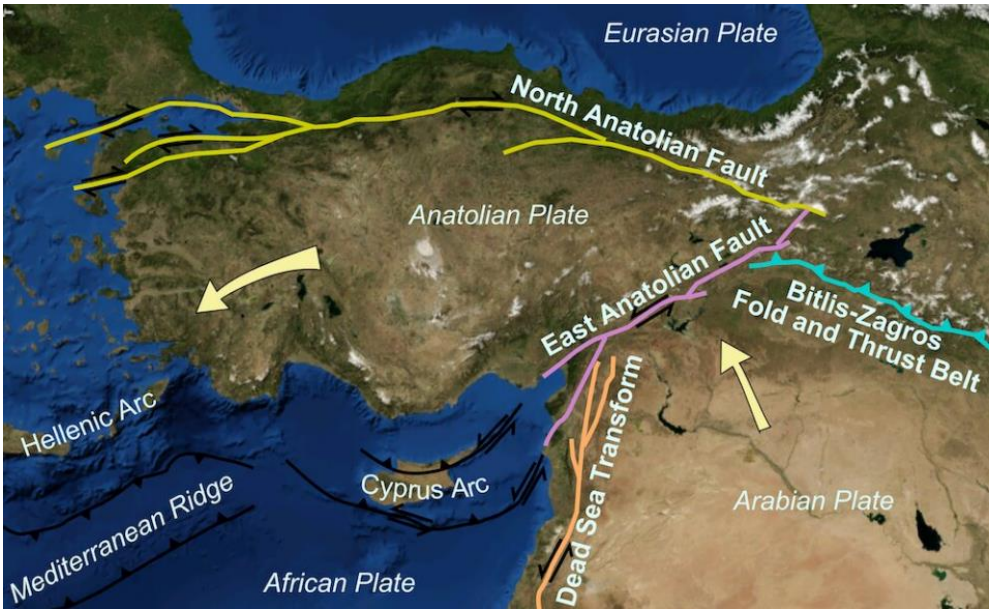

Fig. 1 The geological structure of the Anatolian plate (Erdik et al., 2023).

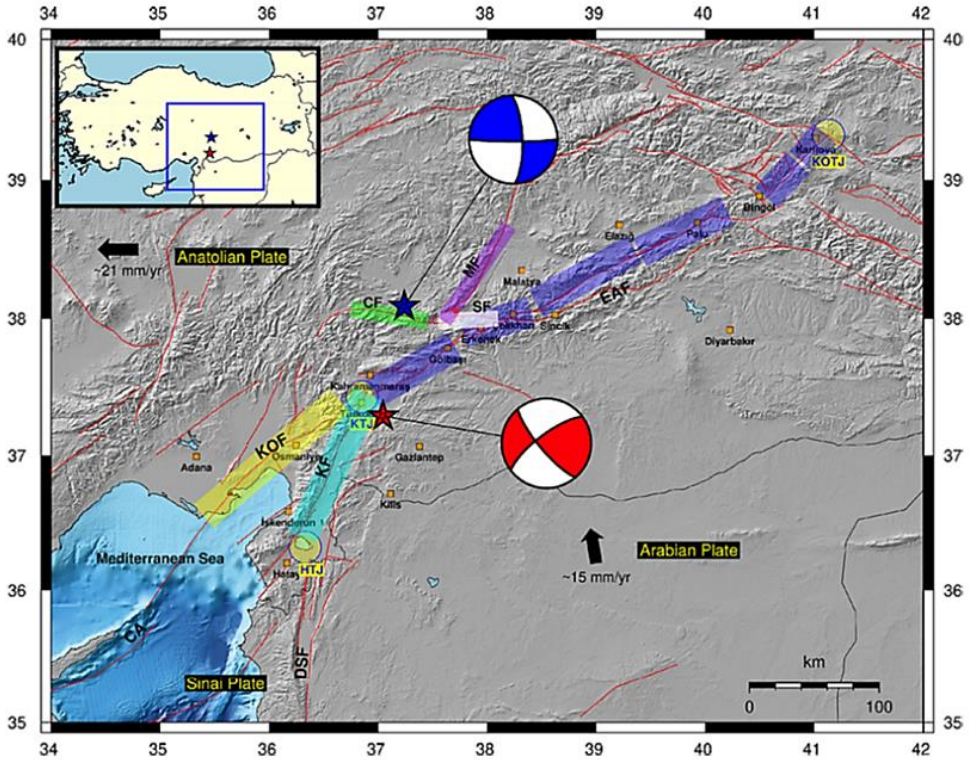

Fig. 2 The focal mechanism of the 6 February Turkey earthquakes (Erdik et al., 2023).

It was investigated the source characteristics, ground motions, and casualty estimates of the 2023 Mw 7.8 and 7.5 Turkey earthquakes (Chen et al., 2022). Using the back-projection technique and seismic data from Alaskan and Canadian stations, they resolved the rupture processes of both events. Aftershocks that occurred during the first day following the Mw 7.8 earthquake displayed fault patterns highly consistent with the back-projection results (Chen and Zebker, 2000; Şengör et al., 2019). Their findings revealed that the Mw 7.8 event ruptured bilaterally toward the northeast and southwest over lengths of approximately 140 km and 130 km, respectively (Şengör et al., 2019). The rupture length and duration were estimated at ~270 km and 80 s. The back-projection also showed that the eastern segment of the rupture was clearly imaged, while the western segment was less well defined (Chen et al., 2022). In

another attempt to analyze the complex dynamics of the 2023 Kahramanmaraş earthquake doublet (Mw 7.8–7.7), it was examined rupture paths using combined near-field and far-field seismic and geodetic observations, together with data-driven models and physics-based rupture simulations (Chen et al., 2023; Styron and Pagani, 2020). Their study demonstrated that compressional, interactive, and both static and dynamic triggering processes operated across a complex fault system, generating a cascade of ruptures with an unusually long cumulative rupture length and high seismic moment. They concluded that physics-based approaches, while powerful, can sometimes yield inconsistent interpretations when constrained by limited near-field observations. Thus, reassessing commonly used assumptions in earthquake hazard assessments is necessary (Jia et al., 2023).

Furthermore, the post-seismic deformation and the transition back to the interseismic phase—during which strain re-accumulates on fault segments—should be closely monitored using long-term GNSS stations, repeated GNSS campaigns, and seismic modeling studies to better understand tectonic processes in the region (Özkan et al., 2023). It has been characterized the rupture geometry and slip distribution of the Kahramanmaraş earthquakes (Mw 7.7 and Mw 7.6) using a dense GNSS network (Erdik et al., 2023; Styron and Pagani, 2020). This high-resolution array included 113 sites, comprising both permanent GNSS stations and campaign observation sites. Inversion modeling of the surface displacements in an elastic half-space was applied to predict co-seismic displacements at these sites. The inversion procedure was performed in two stages: first, by modeling the fault geometry with uniform slip, and second, by estimating slip vectors across discretized patches on the fault plane while refining the fault geometry (Erdik et al., 2023).

It was investigated coseismic deformation, fault slip distribution, and Coulomb stress perturbations of the 2023 Turkey–Syria earthquake doublet using SAR offset tracking (Özkan et al., 2023). Their analysis addressed the limitations of conventional seismic observations by incorporating rupture geometry derived from surface deformation and applying Coulomb stress modeling to evaluate interactions between the main earthquakes, adjacent faults, and regional stress transfer (Wang et al., 2023). The main conclusions of their study can be summarized as follows:

- The D-InSAR approach was hampered by poor surface coherence, whereas SAR offset tracking performed well and provided reliable deformation measurements.
- The deformation associated with the Mw 7.6 earthquake was slightly greater than that of the Mw 7.8 event. In addition, ascending-track observations revealed larger displacements compared with the descending-track data at corresponding locations.
- Both earthquakes exhibited left-lateral strike-slip motion, with slip depths reaching up to 20 km. The Mw 7.8 event generated slips mainly in the eastern and central segments of the southeastern East Anatolian Fault Zone (EAFZ), whereas the Mw 7.6 rupture occurred in the western segment of the northern EAFZ (Xu et al., 2020).
- The Mw 7.8 earthquake likely triggered the Mw 7.6 event, which in turn inhibited slip in the central portion (S2) of the southern EAFZ (Goldstein and Werner, 1998; Mai et al., 2023).
- Coulomb stress modeling of the Mw 7.6 event indicated stress increases on several neighboring structures. These findings emphasize the complexity of the 2023 earthquake sequence and highlight the need for additional near-field observations to clarify the relationship between slip distribution and stress transfer (Ramirez et al., 2020).

Overall, the study underlines the importance of combining SAR offset tracking with Coulomb stress modeling to better understand fault interactions and assess seismic hazards in the East Anatolian Fault Zone (Wang et al., 2023).

In this paper, we aim to compare the effects of crustal deformation associated with the 2023 Turkey earthquakes on northern Egypt and Turkey. Our objective is to assess the seismic risk posed by Mediterranean earthquakes in northern Egypt. To achieve this, we employ data from GNSS and InSAR (Interferometric Synthetic Aperture Radar) observations.

METHODOLOGY

Currently, GNSS technology has been developed for mapping and surveying tasks such as real-time deformation monitoring, setting out surveys, and camera positioning for aerial photography. Today, the most widely used positioning techniques rely on satellites. However, a variety of factors—including satellite geometry, receiver quality, and climatic conditions—can affect the positional accuracy achieved by these systems. Numerous error sources must be considered and simulated in geodetic, geodynamic, and deformation analysis studies, particularly for regional and international implementations of the PPP (Precise Point Positioning) technique. As a result, primary error sources that previously affected GPS measurements—such as multipath effects, antenna phase center offsets, and ionospheric and tropospheric delays—have been significantly reduced (Saraçoğlu, 2024). Among the many fundamental causes of these errors, seasonal changes remain the most significant. One of the most important seasonal variations is deformation related to earthquake activity.

Crustal movement studies are essential for understanding the Earth's geodynamics at regional and local scales. In this research, GNSS data were used to investigate the co-seismic deformation resulting

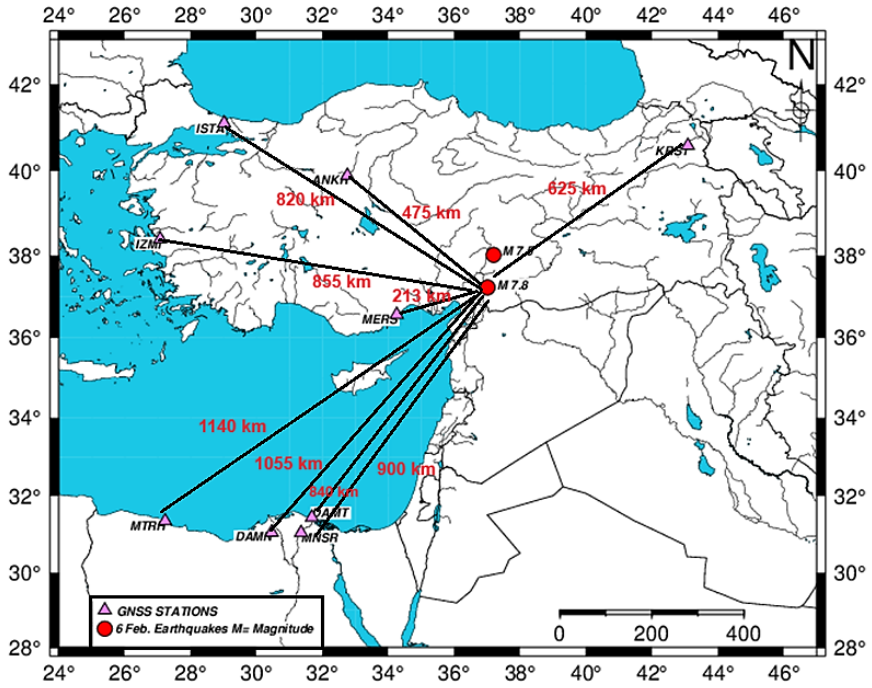

Fig. 3 Distribution of used GNSS stations around 6 Feb., Earthquakes, and baseline lengths.

from the Turkey earthquake of 6 February 2023. Several stations in Turkey (ANKR, ISTA, IZMI, KRS1, and MERS) were analyzed from 24 January 2023 to 25 February 2023.

In Egypt, the study aimed to evaluate the potential impact of the Turkey earthquake on northern Egypt in 2023. The National Research Institute of Astronomy and Geophysics (NRIAG) has been monitoring crustal deformation in Egypt using the Egyptian Permanent GNSS Network (EPGN), which consists of approximately 34 GNSS stations that continuously record observations. For this study, data from EPGN stations located in northern Egypt (BORG, DAMN, DAMT, EDFN, and MTRH) were used. The same period, from 24 January 2023 to 25 February 2023, was analyzed for time series deformation studies at these stations. All GNSS data were processed using Bernese v.5.2 (Chen et al., 2022), and daily solutions were computed. High-precision GNSS observations from permanent and campaign stations were used to determine the deformation. Data were recorded continuously at 1-second intervals over 24-hour periods, enabling millimeter-level positioning accuracy and detailed monitoring of crustal motion. Observations throughout the seismic cycle also allow the assessment of active deformation rates and depth-dependent fault properties. The GNSS data were processed using a systematic computational approach. The ITRF2014 reference frame was adopted, along with IGS final orbits, satellite clock corrections, and Earth orientation parameters. Phase observations were analyzed, and automatic baseline formation was performed using the OBS-MAX technique, which selects the maximum number of observations. In the post-processing stage, normal equations from daily solutions were combined using ADDNEQ2 to produce final coordinate solutions for each campaign.

The baseline solution generated coordinate and variance–covariance files for each baseline. After filtering the observation files and resolving most ambiguities to integer values, the final fixed ambiguity solution was estimated. To define the reference frame, three no-net-translation and three no-net-rotation constraints were applied. This approach allowed precise estimation of horizontal and vertical coordinates at all stations, providing a detailed understanding of crustal motion across the network.

The baseline length between earthquake epicenters and GNSS stations in Turkey varies between 213 km at the MERS station and 855 km at IZMI. While in Egypt, the average baseline length is 1000 km, as shown in Figure 3. The distance from the earthquake epicenter plays an important role in crustal deformation associated with the earthquake. In addition to the GNSS tool, **Interferometric Synthetic Aperture Radar (InSAR)** is an active (independent) remote sensing technology that can map surface topography with an accuracy of a few meters and detect ground crustal deformation at the millimeter level. InSAR can image and cover wide areas under all weather conditions over periods ranging from days to years. Whether space-borne or airborne, SAR systems have a side-looking antenna that scans the Earth's surface using microwave radar along a path parallel to the sensor’s flight direction. It has been successfully used worldwide, for example, to map the Earth’s surface, measure crustal deformation, calculate ground displacements due to earthquakes (Abdelaal et al., 2025; Bao et al., 2025; Saleh et al., 2023), monitor

Table 1 Parameters of the Sentinel-1 SAR scenes.

Track	Master	Slave	Baseline (m.)	Heading/Incidence angle (°)
ASC-14	2023-01-28	2023-02-09	175	−13/34.2
DES-21	2023-01-29	2023-02-10	103	−167/34

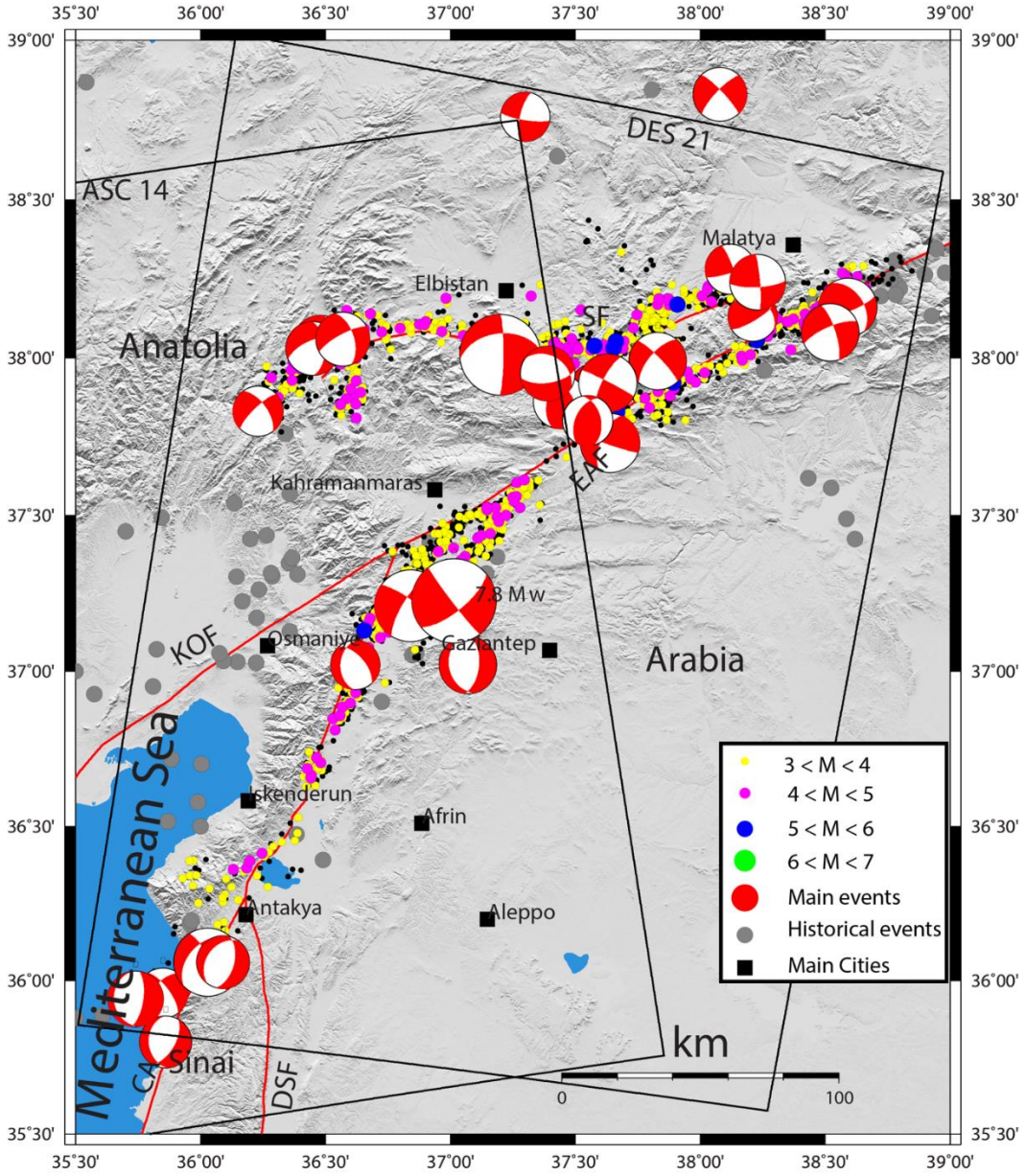

Fig. 4 The earthquake area with the focal mechanisms for both events in the earthquake doublet, in addition to the aftershocks. Plate boundaries are in red. Known and mapped fault surface traces are shown as dark grey lines. Rectangular represents the ascending and descending tracks of the Sentinel-1 mission.

active volcanoes, observe glacier dynamics, and detect land subsidence (Abo Gharbia et al., 2024) (Esmaeel et al., 2025; Hassan et al., 2025; Nabil et al., 2025; Saleh and Becker, 2019).

In the case of studying crustal movements caused by major earthquakes, data from before and after the earthquake are analyzed, with all necessary corrections applied for atmospheric effects and the topography of the study area, in addition to using precise satellite orbit data. For the estimation of co-seismic deformation of the 2023 earthquake doublet at the border between Turkey and Syria, we utilized the Single-Look Complex (SLC) of Sentinel-1 scenes from both ascending (ASC-14) and descending (DES-T21) tracks, covering the study area (Table 1) as shown in Figure 4. The Sentinel-1 SAR mission consists of two satellites, 1A and 1B, which were launched on April 3, 2014, and April 22, 2016,

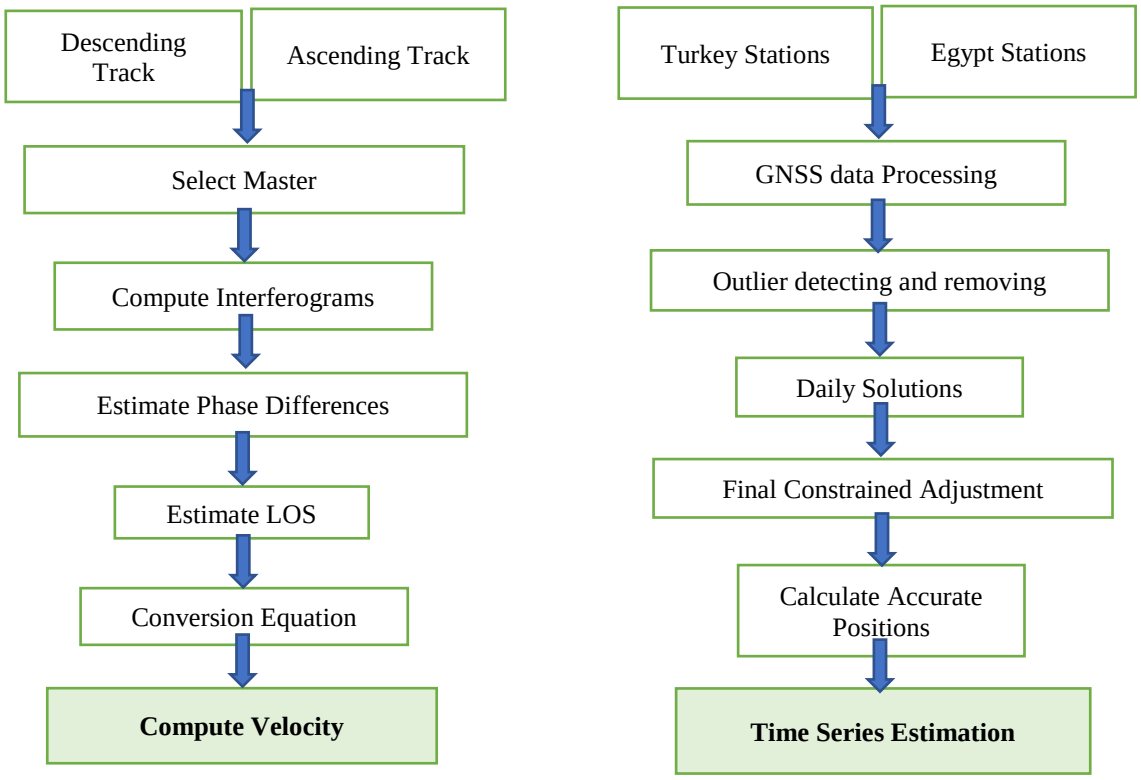

Fig. 5 Flow chart for InSAR and GNSS data Processing Stages.

respectively. Both satellites are orbiting the Earth in the same orbit with a temporal resolution of 12 days, giving an observation for the same area on the Earth every 6 days (Delouis et al., 2023). The Sentinel-1 mission is working in the C-band with a wavelength of 5.6 cm (Xu et al., 2020).

The Sentinel-1 SAR data were processed using the open-source InSAR processing tool GMTSAR (Sandwell et al., 2011). The differential InSAR applied to SAR scenes collected from both ascending and descending tracks, ASC-14 and DES-21, respectively. To account for the phase shift contributed from the topographic signal, we utilized the 30 m spatial resolution Digital Elevation Model (DEM) from the Shuttle Radar Topography Mission (SRTM) (Farr et al., 2007). The interferogram was generated by applying the double-difference technique, which enhanced the accuracy of terrain-induced phase variations. Precise Orbit Data (POD) from the European Space Agency (ESA) is used to correct for the orbital issues. The interferograms were multi-looked using the 3:1 ratio between the range and azimuth directions. A 200 m Gaussian filter is used to filter the phase, employing an adaptive algorithm (Ramirez et al., 2020). Then, the phase was unwrapped using the Statistical-cost, Network-flow Algorithm for Phase Unwrapping (SNAPHU) package to resolve phase ambiguities (Chen and Zebker, 2000). After correction, the unwrapped phase was converted to the Line Of Sight (LOS) displacements and geocoded to WGS-84 using a 30 m-DEM resolution. Figure 5 shows the processing workflow used in this work for handling both GNSS and InSAR data.

RESULTS AND DISCUSSION

In this study, two types of geodetic data were utilized: GNSS and InSAR. GNSS data covering 30 days before, during, and after the Turkey earthquakes were analyzed and processed using Bernese v.5.2 software. Data from IGS stations in Turkey were used to evaluate the crustal deformation effects of the earthquakes in the region. These stations include MERS, ANKR, IZMI, ISTA, and KRS1 (Fig. 6). In Egypt, data from the Egyptian Permanent Geodetic Network (EPGN) were employed to investigate geodynamic responses related to the Turkey earthquakes. Four EPGN stations distributed along northern Egypt were selected for analysis: DAMN, MTRH, DAMT, and MANS.

As shown in Figure 6, GNSS time series analysis reveals displacements associated with the 6 February 2023 earthquakes in Turkey GNSS stations. Also, Table 2 shows the displacements in Easting, Northing, and Height. Small displacements are observed at the MERS and ANKR stations, particularly before and after the earthquakes. In contrast, other stations (KRS1, IZMI, and ISTA) did not exhibit comparable displacement, likely due to their greater distance from the earthquake epicenters. Furthermore, the displacements are predominantly horizontal rather than vertical, which is consistent with the strike-slip mechanism of the East Anatolian Fault system

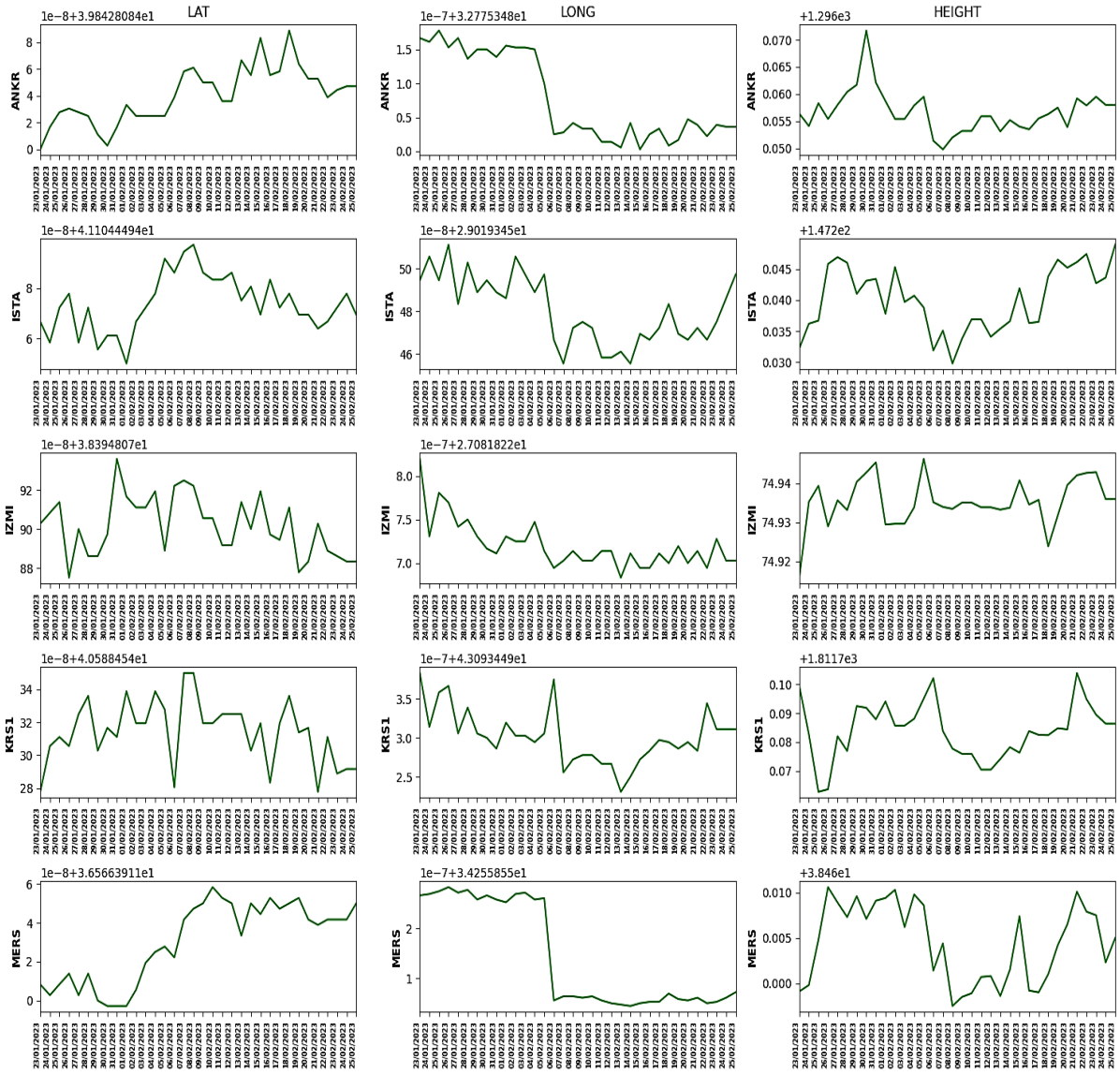

Fig. 6 Time series of GNSS stations in Turkey.

Table 2 Displacement in E, N, and H for Turkey stations.

Station	Displacement in E	Displacement in N	Displacement in H	RMS in E	RMS in N	RMS in H
ANKR	-0.0040	0.0002	-0.0056	0.002	0.004	0.005
MERS	-0.0075	-0.0012	-0.0036	0.001	0.003	0.004
ISTA	-0.0011	0.0016	-0.0081	0.004	0.003	0.004
IZMI	-0.0022	0.0023	-0.0002	0.003	0.001	0.006
KRS1	0.0007	-0.0009	0.0001	0.002	0.003	0.006

For the estimation of co-seismic deformation of the 2023 earthquake doublet at the border between Turkey and Syria, we utilized the Single-Look Complex (SLC) of Sentinel-1 scenes from both ascending (ASC-14) and descending (DES-T21) tracks, covering the study area (Table 2). Based on the Differential InSAR (D-InSAR) analysis for the scenes selected from both ascending and descending tracks, the resulting interferograms from both tracks, derived from LOS displacement are presented in Figure 7. The estimated co-seismic LOS displacement from both ascending and descending tracks for the 2023 earthquake doublet at the border between Turkey and Syria is extending from the Dead Sea Fault (DSF) in the south to the East Anatolian Fault (EAF) in the north (approximately 400 km.). The interferograms in Figures 2A and 2B shows a decorrelation in the near fault regions due to the mass destruction and high

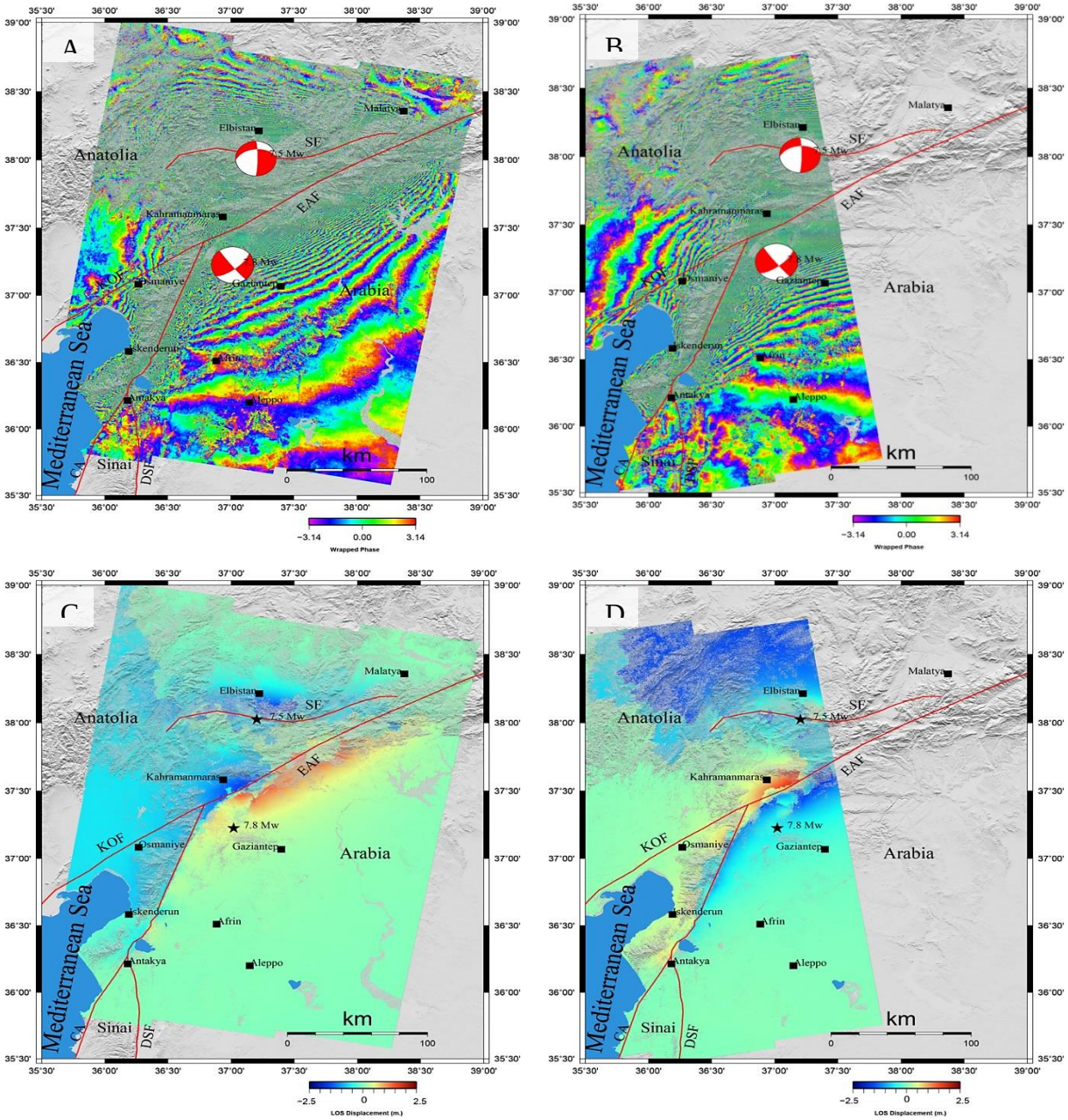

Fig. 7 Interferograms and co-seismic LOS displacement for the 2023 earthquake doublet at the border between Turkey and Syria: (a,c) Interferograms recorded by the Sentinel 1 satellite for descending or rising orbits. The most important event is indicated by the black star. The red line indicates an important mistake in the inspection area. Beach ball. (b,d) Co-geometric loss shifts estimated from descending or rising trajectories.

displacement values close to the fault. Figures 2C and 2D show the co-seismic deformation associated with 7.8 Mw and 7.6 Mw earthquakes. Even with the decorrelation effects, co-seismic deformation of 5 m. is estimated. Since D-InSAR is sensitive to the movements in the LOS, the difference in sign for the LOS displacements between ascending and descending track indicate that the majority of the deformation along these faults is of strike-slip nature which is consisting with the focal mechanism solutions for both events and aftershocks in addition to the regional tectonics of the region.

The deformation associated with the 3 February earthquakes shows damage near the epicenter, while GNSS stations away from the earthquake source show insignificant displacements. On the other hand, in Egypt, the GNSS data time series showed a tendency to decrease in the heights of points MTRH, MNSR, and DAMT before the earthquake events. The horizontal time series does not show a certain trend in the behavior of displacements before, during, and after the 6 February earthquakes. All stations show small displacements that may be attributed to the local structural system controlling the area. So, we can

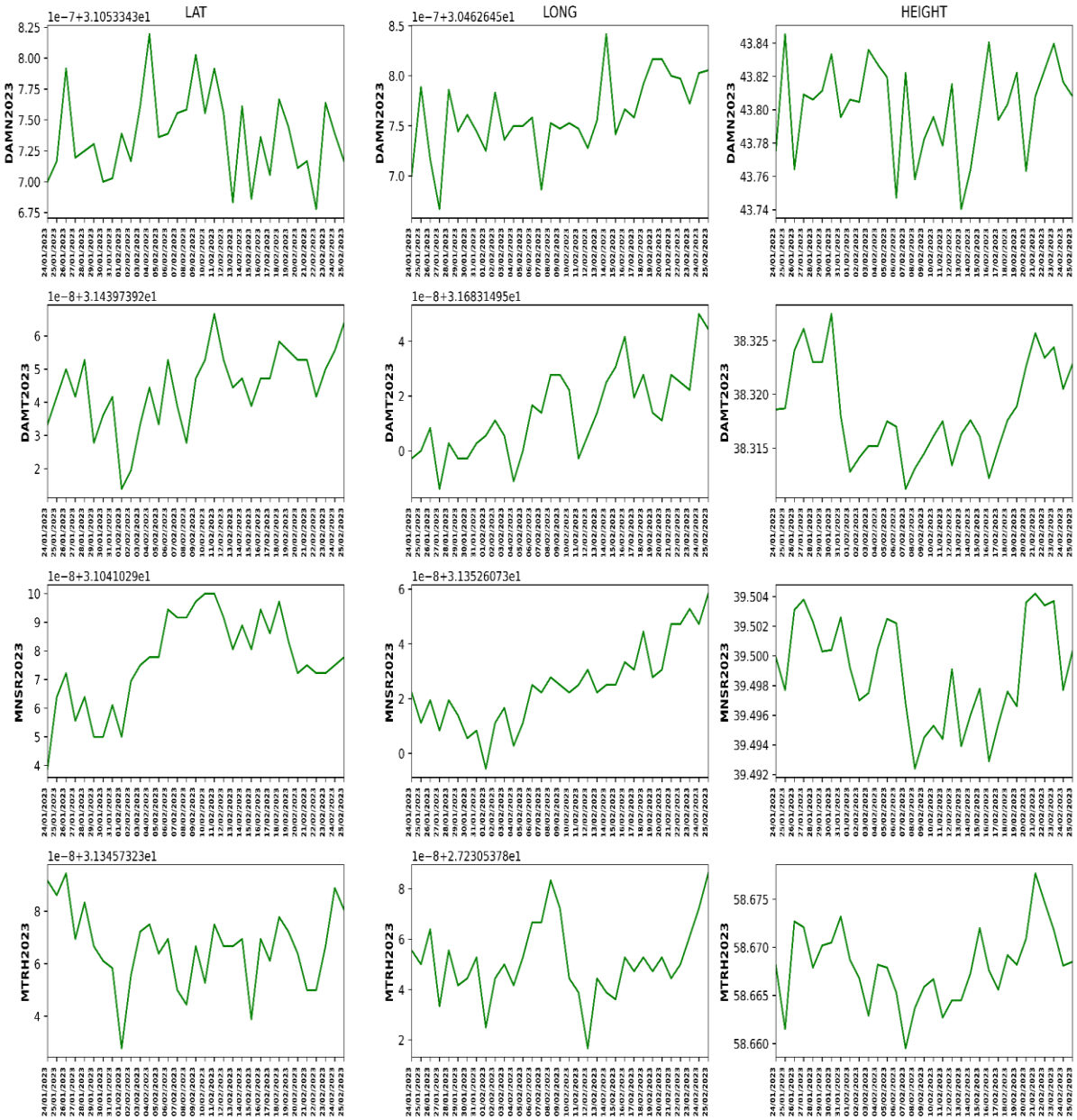

Fig. 8 Time series of GNSS stations in Egypt.

Table 3 Displacement in E, N, and H for Egypt stations.

Station	Displacement in E	Displacement in N	Displacement in H	RMS in E	RMS in N	RMS in H
MNSR	0.0005	0.0010	-0.0031	0.002	0.004	0.006
DAMN	-0.0001	0.0000	-0.0054	0.002	0.004	0.005
DAMT	0.0005	0.0010	-0.0015	0.005	0.003	0.008
MTRH	0.0019	0.0007	-0.0031	0.003	0.005	0.006

suggest that the Northern part of Egypt represents a stable area that is not affected by earthquakes in the Turkey region because the geological structure feature between the north of Egypt and the Anatolian Plate is different (see Fig. 8 and Table 3).

The earthquake activity from 01-01-2023 to 01-03-2023 has been investigated along the northern part of Egypt (Fig. 9). An earthquake with a magnitude of 4.1 along the Dead Sea Fault system happened on 7 February 2023. This earthquake is related to the 6 February Turkey earthquake. The Dead Sea fault system is directly connected with the East Anatolian Fault System. So, any activity in the Anatolian region can be reflected in the Dead Sea fault area. But in Egypt, there was no earthquake activity before or after the 6 February earthquake. This supports the idea that displacement in the northern part of Egypt was not affected by the 6 February earthquakes.

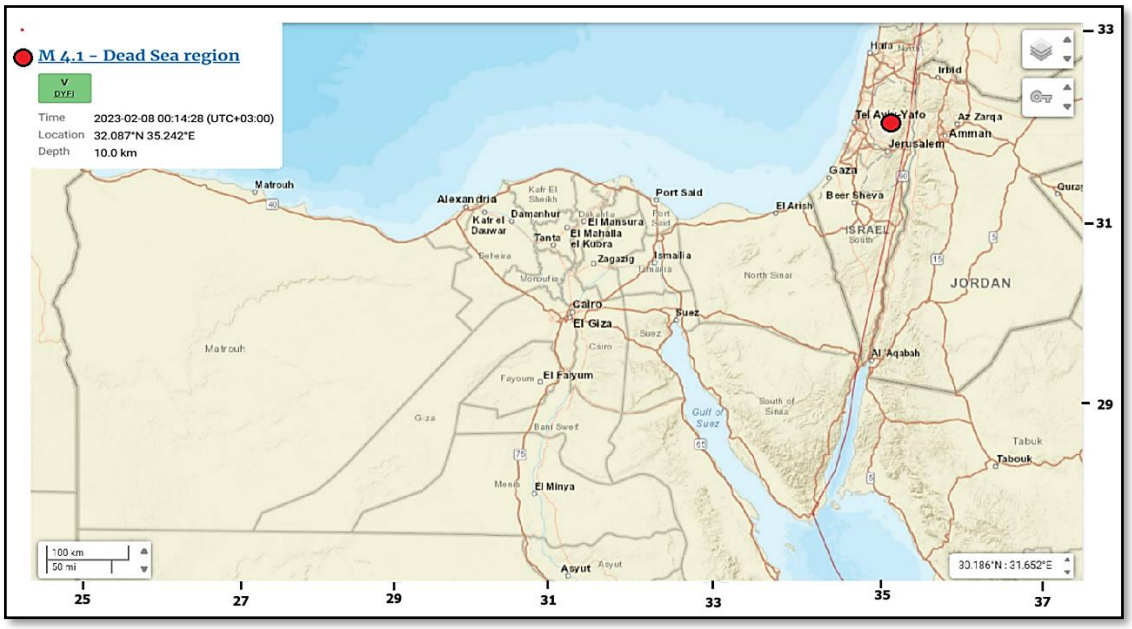

Fig. 9 Earthquake activities in northern Egypt from 01-01-2023 to 01-03-2023 from the United tates Geological Survey (USGS) catalog.

CONCLUSION

The 6 February 2023 earthquake occurred along the East Anatolian Fault system, causing catastrophic damage to property and loss of life. The effects of such large earthquakes can extend hundreds of kilometers, potentially inducing deformation in northern Egypt. This study investigates the deformation associated with the 6 February earthquake in both Egypt and Turkey.

GNSS and InSAR observations were used for this analysis. InSAR results indicate deformation of up to 5 m near the earthquake epicenters in Turkey. Time series analysis of GNSS data shows significant displacement at the MERS station in Turkey, while other stations exhibited minimal deformation due to their distance from the epicenters.

In Egypt, GNSS time series indicate no significant deformation, suggesting only local displacements. No clear correlation was observed between local deformation in northern Egypt and the 6 February earthquake in Turkey. Furthermore, no seismic activity was recorded along northern Egypt during this period. These findings suggest that the deformation from the 6 February 2023 earthquake did not reach the Egyptian coastline. Large earthquakes in the eastern Mediterranean can, however, generate tsunamis, which may raise sea levels and threaten coastal areas.

It is therefore recommended to establish an integrated early warning system along the northern Egyptian coast, combining tide gauges, GNSS, and seismic stations to enhance monitoring and disaster preparedness.

REFERENCES

Abdelaal, M.I., Bao, M.,Saleh, M. and Xing, M.: 2025, New insights into the Menyuan Ms6.9 Earthquake, China: 3D slip inversion and fault modeling based on InSAR remote sensing approach. Egypt. J. Remote Sens. Space Sci., 28, 1, 116–127. DOI: 10.1016/j.ejrs.2024.11.003

Abo Gharbia, A.Y., Saleh, M., Gomaa, A., Mousa, A.E., Hassan, M.R. and Abbas, I.A.: 2024, A 2D velocity field computation using multi-dimensional InSAR: A case study of the Abu-Dabbab area in Egypt. J. Appl. Geod., 19, 3. DOI: 10.1515/jag-2024-0088

Bao, M., Abdelaal, M.I., Saleh, M., Chourak, M., Mohamed, M. and Xing, M.: 2025, Unlocking the hidden secrets of the 2023 Al Haouz earthquake: Coseismic model reveals intraplate reverse faulting in Morocco derived from SAR and seismic data. Int. J. Appl. Earth Obs. Geoinf., 137, 104420. DOI: 10.1016/j.jag.2025.104420

Chen, C.W. and Zebker, H.A.: 2000, Network approaches to two-dimensional phase unwrapping: intractability and two new algorithms. J. Opt. Soc. Am. A, 17, 3, 401–414. DOI: 10.1364/JOSAA.17.000401

Chen, W. et al.: 2022, Rapid estimation of seismic intensities using a new algorithm that incorporates array technologies and ground-motion prediction equations (GMPEs). Bull. Seismol. Soc. Am., 112, 3, 1647–1661. DOI: 10.1785/0120210207

Chen, W. et al.: 2023, Early report of the source characteristics, ground motions, and casualty estimates of the 2023 Mw 7.8 and 7.5 Turkey earthquakes. J. Earth Sci., 34, 2, 297–303. DOI: 10.1007/s12583-023-1316-6

Delouis, B., van den Ende, M. and Ampuero, J.-P.: 2023, Kinematic rupture model of the February 6th 2023 Mw7. 8 Turkey earthquake from a large set of near-source strong motion records combined by GNSS offsets reveals intermittent supershear rupture. DOI: 10.22541/essoar.168286647.71550161/v1

Erdik, M. et al.: 2023, A preliminary report on the February 6, 2023 earthquakes in Türkiye. Research Briefs. DOI: 10.32858/temblor.297

Esmaeel, S.M, Saleh, M., Ali, H.E., Khalil, E., Ahmed, S.M. and Abdel-Wahab, A.M.: 2025, Enhancing monitoring flash flood dams: A cost-effective approach for post-storm assessment using remote sensing. Ain Shams Eng. J., 16, 8, 103493. DOI: 10.1016/j.asej.2025.103493

Farr, T.G. et al.: 2007, The shuttle radar topography mission. Rev. Geophys., 45, 2. DOI: 10.1029/2005RG000183

Goldstein, R.M. and Werner, C.L.: 1998, Radar interferogram filtering for geophysical applications. Geophys. Res. Lett., 25, 21, 4035–4038. DOI: 10.1029/1998GL900033

Gunaydin, O. et al.: 2023, Fault displacement analysis using a multidisciplinary approach on the Gerede Segment of the North Anatolian Fault Zone. Soil Dyn. Earthq. Eng., 164, 107519. DOI: 10.1016/j.soildyn.2022.107519

Hassan, S., Saleh, M., Mohamed, B., Elhebiry, M.S., Abdeldayem, A., Issawy, E., Zahran, K. and Kamh, S.: 2025, Environmental risk assessment of the Nile Delta, Egypt, based on radar interferometry, altimetry, and geodetic measurements. Sci. Rep., 15, 19209. DOI: 10.1038/s41598-025-03831-w

Jia, Z. et al.: 2023, The complex dynamics of the 2023 Kahramanmaraş, Turkey, M w 7.8-7.7 earthquake doublet. Science, 381, 6661, 985–990. DOI: 0.1126/science.adi0685

Li, S. et al.: Source model of the 2023 Turkey earthquake sequence imaged by Sentinel-1 and GPS measurements: implications for heterogeneous fault behavior along the East Anatolian Fault Zone. Remote Sens., 15, 10, 2618. DOI: 10.3390/rs15102618

Liu, J. et al.: 2024, Immature characteristics of the East Anatolian Fault Zone from SAR, GNSS and strong motion data of the 2023 Türkiye–Syria earthquake doublet. Sci. Rep., 14, 1, 10625. DOI: 10.1038/s41598-024-61326-6

Mai, P.M. et al.: 2023, The destructive earthquake doublet of 6 February 2023 in south-central Türkiye and northwestern Syria: Initial observations and analyses. Seism. Rec., 3, 2, 105–115. DOI: 10.1785/0320230007

Melgar, D. et al.: 2023, Sub-and super-shear ruptures during the 2023 Mw 7.8 and Mw 7.6 earthquake doublet in SE Türkiye. Seismica, 2, 3. DOI: 10.26443/seismica.v2i3.387

Nabil, A., El-Ashquer, M., Saleh, M., Mousa, A.E.-K. and El-Fiky, G.S.: 2025, Crustal deformation in East of Cairo, Egypt, induced by rapid urbanization, as seen from remote sensing and GNSS data. J. Appl. Geod, 19, 2. DOI: 10.1515/jag-2024-0094

Özkan, A. et al.: 2023, Characterization of the co-seismic pattern and slip distribution of the February 06, 2023, Kahramanmaraş (Turkey) earthquakes (Mw 7.7 and Mw 7.6) with a dense GNSS network. Tectonophysics, 866, 230041. DOI: 10.1016/j.tecto.2023.230041

Potin, P. et al.: 2016, Sentinel-1 mission status. In: Proceedings of EUSAR 2016: 11th European Conference on Synthetic Aperture Radar, Hamburg. https://ieeexplore.ieee.org/xpl/conhome/7559229/proceeding

Ramirez, R., Lee, S.-R. and Kwon, T.-H.: 2020, Long-term remote monitoring of ground deformation using Sentinel-1 interferometric synthetic aperture radar (InSAR): Applications and insights into geotechnical engineering practices. Appl. Sci., 10, 21, 7447. DOI: 10.3390/app10217447

Saleh, M. and Becker, M.: 2019, New estimation of Nile Delta subsidence rates from InSAR and GPS analysis. Environ. Earth Sci., 78, 6. DOI: 10.1007/s12665-018-8001-6

Saleh, M., Meghraoui, M. and Cetin, E.: 2023, The 12 November 2017 Mw 7.4 earthquake in Sarpol-e-Zahab (Iran–Iraq): a complex fault rupture in the Zagros Mountains. Med. Geosc. Rev., 5, 177–188. DOI: 10.1007/s42990-023-00107-1

Sandwell, D. et al.: 2011, GMTSAR: An InSAR processing system based on generic mapping tools. Lawrence Livermore National Laboratory, Livermore. https://escholarship.org/uc/item/8zq2c02m

Saraçoğlu, A.: 2024, Causal insights into GPS precision variability: an investigation into the ionospheric impact on GPS measurements throughout the solar cycle. Bull. Geophys. Oceanogr., 65, 1. DOI: 10.4430/bgo00438

Şengör, A.C., Zabcı, C. and Natalin, B.A.: 2019, Continental transform faults: Congruence and incongruence with normal plate kinematics: In: Transform plate boundaries and fracture zones. Elsevier, 169–247. DOI: 10.1016/B978-0-12-812064-4.00009-8

Styron, R. and Pagani, M.: 2020, The GEM global active faults database. Earthq. Spectra, 36, 3, 160–180. DOI: 10.1177/8755293020944182

Wang, W. et al.: 2023, Coseismic deformation, fault slip distribution, and coulomb stress perturbation of the 2023 Türkiye-Syria Earthquake doublet based on SAR offset tracking. Remote Sens., 15, 23, 5443. DOI: 10.3390/rs15235443

Xu, J., Liu, C. and Xiong, X.: 2020, Source process of the 24 January 2020 Mw 6.7 East Anatolian fault zone, Turkey, earthquake. Seismol. Res. Lett., 91, 6, 3120–3128. DOI: 10.1785/0220200124

Zahradník, J., Turhan, F., Sokos, E. and Gallovič, F.: 2023, Asperity-like (segmented) structure of the 6 February 2023 Turkish earthquakes. DOI: 10.31223/X5T666